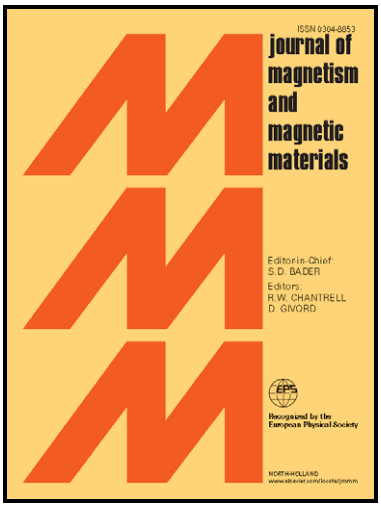

An improved technique for the measurement of the complex susceptibility of magnetic colloids in the microwave region

P.C. Fannin, C. MacOireachtaigh, C. Couper

PII: S0304-8853(10)00158-7
DOI: doi:10.1016/j.jmmm.2010.02.051
Reference: MAGMA 56138

To appear in: *Journal of Magnetism and Magnetic Materials*

Received date: 12 November 2009
Revised date: 17 February 2010
Accepted date: 24 February 2010

Cite this article as: P.C. Fannin, C. MacOireachtaigh and C. Couper, An improved technique for the measurement of the complex susceptibility of magnetic colloids in the microwave region, *Journal of Magnetism and Magnetic Materials*, doi:10.1016/j.jmmm.2010.02.051

Journal of Magnetism and Magnetic Materials xxx (2008) 0–0

Contents lists available at ScienceDirect

Journal of Magnetism and Magnetic Materials

journal homepage: www.elsevier.com/locate/agee

An improved technique for the measurement of the complex susceptibility of magnetic colloids in the microwave region.

P.C. Fannin*, C. MacOireachtaigh, C. Couper.

Department of Electronic and Electrical Engineering, Trinity College, Dublin 2, Ireland.

ARTICLE INFO

Elsevier use only
Article history:
Received date here
Received in revised form date here
Accepted date here
Available online date here

Keywords: 75.50Mm - Magnetic fluids; 75.40.Gb - Complex magnetic susceptibility; Ferrofluids, Ferromagnetic resonance, Complex Susceptibility, Complex permittivity, Transmission lines.

ABSTRACT

Measurements by means of the short-circuit (S/C) and open circuit (O/C) transmission line techniques, are well established methods for investigating the magnetic and dielectric properties of magnetic colloids, respectively. In particular, the S/C technique has been used in the investigation of the resonant properties of ferrofluids; resonance being indicated by the transition of the real component of the magnetic complex susceptibility, $\chi(\omega) = \chi'(\omega) - i\chi''(\omega)$, from a +ve to a –ve value at a frequency, f_{res}.
However, under certain circumstances, the accuracy of the S/C technique is affected by the dielectric properties of the sample, hence incurring errors in the measurement of $\chi(\omega)$ and indeed of f_{res}. Here we present a model which, by combining short-circuit and open circuit measurements, is developed in a manner in which the permeability, μ and the permittivity, ε, contribute simultaneously to the calculation of $\chi(\omega)$, thereby providing superior experimental results in comparison to those obtained by the S/C technique alone.
For the two ferrofluid samples measured it is demonstrated that the dielectric properties affect the high frequency content of the susceptibility spectrum.

1. Introduction

Ferrofluids are stable colloidal systems consisting of single-domain nanoparticles of ferromagnetic or ferrimagnetic materials dispersed in a carrier liquid and stabilized by a suitable surfactant. The particles have radii ranging from approximately 2-10 nm and when in suspension their magnetic properties can be approximately described by the paramagnetic theory of Langevin. The particles are considered to be in a state of uniform magnetization with a magnetic moment $m = M_S v$, where M_S denotes the saturation magnetization and v is the magnetic volume of the particle.

The magnetic susceptibility, $\chi(\omega) = \chi'(\omega) - i\chi''(\omega)$, of such an assembly of single domain particles can also be described in terms of its parallel, $\chi_{||}(\omega)$, and perpendicular, $\chi_{\perp}(\omega)$, components, with[1]

$$\chi(\omega) = \tfrac{1}{3}(\chi_{||}(\omega) + 2\chi_{\perp}(\omega)), \qquad (1)$$

where $\chi_{||}(\omega)$ is purely relaxational in character and $\chi_{\perp}(\omega)$ is the resonant component.

$\chi_{||}(\omega)$ can be described by the Debye equation $\chi_{||}(\omega) = \frac{\chi_{||}(0)}{1 + i\omega\tau_{||}}$ [2] with ,

where $\chi_{||}(0)$ is the static parallel susceptibility and $\tau_{||}$ is the parallel relaxation time consisting of a combination of Brownian[3] and Néel[4] relaxational components. $\tau_{||}$ is related to the frequency, f_{max}, at which the imaginary component of $\chi''(\omega)$ is a maximum, by the expression, $f_{max} = 1/(2\pi\tau_{||})$.

The perpendicular or transverse susceptibility, $\chi_{\perp}(\omega)$, can have a resonant character[5], whereby precession of the magnetic moment occurs about an easy axis (i.e. the direction of the internal field H_A); the existence of a resonance phenomenon being indicated by a transition in the value of $\chi'(\omega)$ from a + ve to a -ve quantity at a frequency, f_{res}. In equilibrium, the magnetic moment, m, would be directed along this easy axis if it were not for thermal fluctuations. The extent of this disturbance depends on σ. In the case of a small disturbance, the angular resonant frequency, ω_{res}, is given by,

$$\omega_{res} = 2\pi f_{res} = \gamma H_{res} \qquad (2)$$

where γ ($mA^{-1}s^{-1}$) is the gyromagnetic ratio. Applying an external polarising field, H, results in an increase in ω_{res} given by,

$$\omega_{res} = 2\pi f_{res} = \gamma (H + H_A) \qquad (3)$$

Equation (3) is the equation of a straight line and from a plot of f_{res} against H, the value of H_A can be determined from the intercept of the plot with the x-axis whilst γ is determined from the slope .

In this paper we employ the co-axial transmission line technique as first reported by Roberts and von Hippel [6, 7], in the determination of the complex impedance of the magnetic fluid samples. Fig 1, (from Appendix 1) shows an equivalent circuit of a transmission line terminated in a load impedance Z_R. The method [8, 9], uses a 50Ω coaxial line incorporating a co-axial test cell , (which contains the sample under test, Z_R), with inner diameter 3 mm and outer diameter 7 mm. Ferrofluids have an advantage over solids in that they easily fill the coaxial test cell which has almost radial electric field and a concentric magnetic field. Use of standard open and short calibrating components enables accurate measurements to be made without disturbing the sample during the measurement.

Fig 1. Equivalent circuit of a transmission line terminated in a load impedance Z_R. The line has a characteristic impedance Z_0, and propagation constant γ_0

A short circuit tends to produces a maximum magnetic field and a minimum electric field at the sample whilst, in contrast, an open circuit produces a maximum electric field and a minimum magnetic field at the sample.
For good measurement accuracy, the sample depth must be large enough to ensure sufficient interaction of the sample with the measuring signal, whilst also being small enough to ensure the absence of dimensional resonance [10, 11]. Generally speaking, the lower the measurement frequency, the deeper the test cell required.
Considering the case of the short-circuit (S/C) transmission line, as the frequency of measurement increases, the corresponding wavelength decreases, becoming comparable to the dimensions of the test cell sample depth, with the result that the effects of the electric field can no longer be discounted, leading to a decrease in the accuracy of the measurement.

The object of this work is to show how a combination of data obtained from both O/C and S/C measurements can be used to obtain more accurate equations to describe both the permeability, μ(ω) and the permittivity, ε(ω), than are possible by measuring μ(ω) and ε(ω) separately[12]. As $\mu(\omega) = 1 + \chi(\omega)$, the complex components, $\chi'(\omega)$ and $\chi''(\omega)$, are readily determined.

The combined model is a development of the model presented in [8] for the case of then S/C technique alone and is presented in Appendix 1.

2. Combined Method for Measurement

To improve on the S/C model proposed in [8], two sets of impedance measurements are taken, one for an open circuit, (Z_{inoc}), one for the short circuit, (Z_{insc}) and as shown in Appendix 1, the following equations for μ_r and ε_r, are determined for the combined model.

$$\mu_r = \left\{ \left(\frac{Z_0 \tanh(\gamma_0 x) - Z_{insc}}{Z_{insc} \tanh(\gamma_0 x) - Z_0} \times \frac{Z_0 \tanh(\gamma_0 x) - Z_{inoc}}{Z_{inoc} \tanh(\gamma_0 x) - Z_0} \right) \times \left[\frac{1}{\varepsilon_0 \mu_0 \omega^2 d^2} \left\{ \tan^{-1} \left(-i \sqrt{\frac{Z_0 \tanh(\gamma_0 x) - Z_{insc}}{Z_{insc} \tanh(\gamma_0 x) - Z_0} \times \frac{Z_{inoc} \tanh(\gamma_0 x) - Z_0}{Z_0 \tanh(\gamma_0 x) - Z_{inoc}}} \right) \right\}^2 \right] \right\}^{\frac{1}{2}} \quad (4)$$

$$\varepsilon_r = \left\{ \left(\frac{Z_0 \tanh(\gamma_0 x) - Z_{insc}}{Z_{insc} \tanh(\gamma_0 x) - Z_0} \times \frac{Z_0 \tanh(\gamma_0 x) - Z_{inoc}}{Z_{inoc} \tanh(\gamma_0 x) - Z_0} \right) \div \left[\frac{1}{\varepsilon_0 \mu_0 \omega^2 d^2} \left\{ \tan^{-1} \left(-i \sqrt{\frac{Z_0 \tanh(\gamma_0 x) - Z_{insc}}{Z_{insc} \tanh(\gamma_0 x) - Z_0} \times \frac{Z_{inoc} \tanh(\gamma_0 x) - Z_0}{Z_0 \tanh(\gamma_0 x) - Z_{inoc}}} \right) \right\}^2 \right] \right\}^{\frac{1}{2}} \quad (5)$$

where γ_0, the propagation constant=$\alpha_0+i\beta_0$, α_0 is the attenuation factor, Z_0 is the characteristic impedance of the lossless part of the line, Z_{insc} and Z_{inoc} are the input impedances for the open and short circuits.

3. Measurement and Results

For the measurements reported here, a Hewlett-Packard(HP) 50Ω coaxial line incorporating a coaxial cell with 3 mm inner diameter and 7 mm outer diameter was used in conjunction with a HP 8753C and HP 8722D network analyzers. The samples were placed in the coaxial cell and standard HP open-circuit(O/C) and short-circuit(S/C) test devices used as terminations and the input impedance of the line measured in each case. These instruments automatically measure the reflection and transmission characteristics of devices by use of the scattering parameters, S, which are a measure of the power reflected from a load to the power incident on the load. When operating in the one-port mode the S_{11} parameter is measured. Now $S_{11}= (Z_R-Z_0)/(Z_R+Z_0)$, where Z_R is the load impedance and Z_0=50 Ω . The instrument has the facility to convert the S_{11} measurements to the complex components of Z_R by computing the equation, $Z_R = Z_0(1+S_{11})/(1-S_{11})$. Thus in the case of an inductive load it automatically measures the reactive component, X_L and the resistive component R, respectively.

Using the technique presented, measurements were performed on two samples, sample 1 and sample 2. Sample 1 was a 400 G suspension of magnetite particles of mean radius 5 nm, dispersed in an iso-paraffin carrier (fluid 1), measured over the range 100 MHz to 3 GHz using a 9.5 mm dept cell and the HP 8753C network analyzer. Sample 2, was a 600 G suspension of cobalt particles of mean radius 5nm in oil, measured over the range 1 GHz to 16 GHz using a 1.94 mm depth cell and the HP 8722D network analyzer.

For comparison purposes, measurements were performed using both the separate short -circuit method and the combined method as previously. One would expect both methods to provide the same results at the lower frequencies of each range, and because of capacitive effects, the difference between the methods to become significant at the higher ends of each range.

Figure 2 shows a plot of $\chi'(\omega)$ and $\chi''(\omega)$ for sample 1, over the frequency range 100 MHz to 3 GHz. It can be seen that in the case of the combined model a resonance occurs when f_{res}=1.78 GHz, in contrast to the case of the S/C only model where no resonance is displayed. The figure also illustrates the discrepancy between the $\chi''(\omega)$ components.

Fig 3 shows a plot of $\chi'(\omega)$ and $\chi''(\omega)$ for sample 2, over the frequency range 1 GHz to 16 GHz. In this case there is only a slight difference between the f_{res} and f_{max} values obtained for both models, however the major difference lies in the region following the f_{res} point where the $\chi'(\omega)$ profiles differ substantially, with in the case of the S/C only, the profile going from a –ve to a +ve value at a frequency of approx 15 GHz; this latter action being invalid.

Fig.2. Plots of $\chi'(\omega)$ and $\chi''(\omega)$ for sample 1 in the frequency range 100 MHz to 3 GHz.

Fig.3. Plots of $\chi'(\omega)$ and $\chi''(\omega)$ for sample 2 in the frequency range 1 GHz to 16 GHz.

It is very clear from the above results that the accuracy of the S/C measurement technique breaks down at higher frequencies. As expected, the plots of $\chi(\omega)$ are almost identical in the lower frequency sections of the measured frequency range. This is because the wavelength of the frequency of measurement is very much greater than the sample depth at these particular frequencies.

3.1 Polarised Measurements

As indicated in equation (3), application of an external polarising field, H, to a sample, results in an increase in ω_{res} given by, $\omega_{res} = 2\pi f_{res} = \gamma(H+H_A)$.
Equation (3) is the equation of a straight line and from a plot of f_{res} against H , the value of H_A can be determined from the intercept of the plot with the x-axis whilst γ, the gyromagnetic ratio, is determined from the slope .
Sample two was subjected to a polarising field over the approximate range 0-168.5 kA/m, and the results obtained in the case of both models are shown in Fig4(a) for the $\chi'(\omega)$ components and in Fig 4(b) for the $\chi''(\omega)$ components.

Fig. 4(a). Plots of $\chi'(\omega)$ as a function of polarizing field, H, for sample 2 in the frequency range 1 GHz to 16 GHz.

Fig.4 (b) Plots of $\chi''(\omega)$ as a function of polarizing field, H, for sample 2 in the frequency range 1 GHz to 16 GHz.

From Fig.4(a) it is quite clear, in the case of the S/C model that, following the unpolarised f_{res} value of 6.25 GHz, the 'depth' of the resonance, i.e. the depth below the y = 0 axis to which $\chi'(\omega)$ extends to, diminishes with increase in H. Finally at a value of H = 102.4 kA/m, the resonance disappears, at an approximate frequency of 12GHz. This is in stark contrast to the case of the combined model where f_{res} is distinct and well defined over the whole range of H, thereby enabling f_{res} /H to be plotted, as shown in Fig 5, resulting in a value of H_A = 170 kA/m and γ = 2.32 105 $mA^{-1}s^{-1}$, being determined. This data could not have been obtained in the case of the S/C model alone.
Fig 4(b) shows that there is a slight different in the values of f_{max}, with the major difference occurring at high frequencies where the loss ($\chi''(\omega)$) component of the S/C model is greater than that determined by the combined model. This difference could give rise to errors in the determination of parameters which are a function of the χ'' component, such as the tanδ loss factor [13, 14] and the Neel pre-factor, τ_0, [15]

Fig.5. Plots of f_{res} as a function of polarizing field, H, for sample 2 in the range 0-164.5 kA/m.

4. Conclusion

Measurements obtained by means of the short-circuit (S/C) and open circuit (O/C) transmission line techniques, are well established methods for investigating the magnetic and dielectric properties of materials, in particular, ferrofluids. The S/C technique has previously been used in the investigation of the resonant properties of magnetic fluids; resonance being indicated by the transition of the real component of the magnetic complex susceptibility, $\chi(\omega) = \chi'(\omega) - i\chi''(\omega)$, from a +ve to a –ve value at a frequency, $f_{res.}$
However, depending upon the depth of the measurement cell, and the frequency of measurement, the accuracy of the S/C technique is affected by the dielectric properties of the sample, hence incurring errors in the measurement of $\chi(\omega)$ and indeed of f_{res}; as clearly demonstrated in this work.
To overcome this deficiency, a model which is developed in a manner whereby μ and ε contribute simultaneously to the calculation of $\chi(\omega)$, thereby providing superior experimental results in comparison to those obtained by the S/C technique alone, is presented. In the case of sample 2, it is shown how, for polarized measurements, the combined model produces extended f_{res} data thereby enabling data on H_A and γ to be determined; this data would have been impossible to generate had the S/C model alone been used.

Refrences.

[1] M.I. Shliomis and Yu.L. Raikher, IEEE Trans. Magn. Mag. 16, (1980) 237.

[2] P.Debye,1929, Polar Molecules, (New York, The Chemical Catalogue Company).

[3] W.F.Brown, J. Appl. Phys.34, (1963) 1319.

[4] L. Néel, Ann. Géophys. 5 (1949) 99.

[5] L. D. Landau and E. M. Lifshitz, Phys. Z. Sovietunion, **8** (1935) 153

[6] S . Roberts and A.R. von Hippel, J.Appl.Phys. 17, (1943), 610.

[7] M.A. Stuchly and S.S. Stuchly; IEEE Trans. Instrum. Meas., 29,(1980), 176

[8] P.C.Fannin, T.Relihan and S.W. Charles. J.Phys.D:Appl.Phys. 28,(1995), 2003.

[9] P.C.Fannin, 'Wideband Measurement and Analysis Techniques for the Determination of the Frequency-Dependent, Complex Susceptibility', Adv. in Chem.Phys.104,(1998),181.

[10] E.C. Snelling, and A.D.Giles, 1983, ''Ferrites for Inductors and Transformers'', (New York; John Wiley & Sons Inc).

[11] F.G. Brookman, P.H. Dowling & W.G. Steneck, Phys. Rev., 77, (1950), 85.

[12] P.C.Fannin, T.Relihan and S.W. Charles . J.Magn.Magn.Mater. 167, (1997) 247.

[13] P.C Fannin. J.Magn.Magn.Mater. 321, 7 (2009) 850.

[14] R. E. Collin, *Foundations of for microwave Engineering*, McGraw-Hill Inc. 1966.

[15]P.C Fannin, C.N. Marin,C.N, and C.Couper. J.Magn.Magn.Mater. In Press.

Acknowledgements.

Acknowledgement is due to B.K.P.Scaife, T.Relihan, L.Kinsella and A.T.Giannitsis and also to ESA for part funding of this work.

Appendix 1

Model of Combined Measurement Technique

A1 The proposed model is an extension of that presented in [8] for the case of the S/C Coaxial Transmission line.

Consider the following transmission line terminated in a load, Z_R, as shown in Fig 1(A).

Fig 1(A). Equivalent circuit of a transmission line terminated in a load impedance, Z_R.

The line has a characteristic impedance Z_0, propagation constant γ_0. The input impedance, Z_{in}, at a distance x from the load is given by [6]:

$$Z_{in} = \frac{V_{in}}{I_{in}} = \frac{V_R \cosh(\gamma_0 x) + Z_0 I_R \sinh(\gamma_0 x)}{I_R \cosh(\gamma_0 x) + (V_R/Z_0)\sinh(\gamma_0 x)} \quad \text{A1}$$

where $\gamma_0 = \alpha_0 + i\beta_0$. α_0 is the attenuation factor, $\beta_0 = 2\pi/\lambda$ is the phase coefficient and λ is the operating wavelength in the line. In the case where the line has a very low loss, one can assume $\alpha_0 \approx 0$ so that $\gamma_0 = i\beta_0$ and Z_{in}, becomes

$$Z_{\text{in}} = Z_0 \left\{ \frac{Z_R + iZ_0 \tan(\beta_0 x)}{Z_0 + iZ_R \tan(\beta_0 x)} \right\} \quad \text{A2}$$

For the special case where the load is a short i.e. $Z_R = 0$, then the input impedance is,

$$Z_{in} = iZ_0 \tan(\beta_0 x) \quad \text{A3}$$

A2 Measurement of the Complex Permeability.

Consider the case of an air filled coaxial transmission line terminated with a sample of material which is short circuited (S/C). The sample has a thickness or depth d and Z_0 and γ_0 are the characteristic impedance and propagation constant of the air filled line. The S/C ensures that the magnetic field is large and the electric field small within the sample provided that the wavelength within the sample is much greater than the sample thickness.

As shown in [8] the arrangement can be modelled as that of Fig.1A by having the load impedance include the section of line with the sample and shorted at the end.

Now Z_1 and γ_1 are the characteristic impedance and propagation constant of the sample filled line. In this case it cannot be assumed that this section of the line is loss-less so the general equation (eqn (A3)) has to be used. Since the line is shorted then the input impedance, Z_{RSC} , becomes,

$$Z_{RSC} = Z_1 \tanh(\gamma_1 d) \quad \text{A4}$$

The intrinsic impedance Z of a medium is given by $Z = \sqrt{\frac{\mu_1}{\varepsilon_1}}$,

Where μ_1 and ε_1 are the absolute values of complex permeability and permittivity of the medium. The propagation factor of the medium is $\gamma_1 = i\omega\sqrt{\varepsilon_1\mu_1}$, where ω is the angular frequency.

Therefore it follows that $Z = \frac{i\omega\mu_1}{\gamma_1}$ and the characteristic impedance of a coaxial line containing such a medium as the dielectric is given by [8],

$$Z_1 = \frac{1}{2\pi} Z \ln\left(\frac{r_o}{r_i}\right) \quad \text{A5}$$

where r_o is the radius of the outer conductor and r_i is the radius of the inner conductor of the coaxial line. Assuming that $\gamma_1 d << 1$, then $\tanh(\gamma_1 d) \approx \gamma_1 d$ and Z_{RSC} becomes

$$Z_{RSC} = iA_c \omega \mu_1 d \quad \text{A6}$$

Where $A_c = (1/2\pi)\ln(r_o/r_i)$.This result gives us the load impedance, Z_{RSC}, in terms of the permeability of the sample medium.

In [8] it is shown that,

$$Z_{\text{in}} = Z_0 \left\{ \frac{iA_c \omega\mu_1 d + iZ_0 \tan(\beta_0 x)}{Z_0 - A_c \omega\mu_1 d \tan(\beta_0 x)} \right\}. \quad \text{A7}$$

Which, upon elimination of A_C, gives the relative permeability, μ_r, of the sample medium as,

$$\frac{\mu_1}{\mu_0} = \frac{\lambda}{2\pi d} \left\{ \frac{(Z_{\text{in}}/Z_0) - i\tan(\beta_0 x)}{(Z_{\text{in}}/Z_0)\tan(\beta_0 x) + i} \right\} = \mu_r \quad \text{A8}$$

A3 Measurement of Complex Permittivity.

To measure the complex permittivity of a medium one places the sample at the end of the coaxial line as before but this time the line is terminated by an open circuit (O/C). This ensures that the electric field is large and the magnetic field small within the sample, provided that the wavelength within the sample is much greater than the sample thickness.

Following the procedure used in determining μ_r, one readily obtains the following for the load impedance

$$Z_{ROC} = A_c \frac{\gamma_1}{i\omega\varepsilon_1} \coth(\gamma_1 d) \quad \text{A9}$$

Again making the assumption that the sample depth is much less than the wavelength in the sample so that $\coth(\gamma_1 d) \approx 1/\gamma_1 d$, eqn (A9) becomes

$$Z_{ROC} = Z_1 \coth(\gamma_1 d) \quad \text{A10}$$

Substituting eqn (A10) into eqn (A2) one obtains the following for the input impedance,

$$Z_{\text{in}} = Z_0 \left\{ \frac{(A_c/i\omega\varepsilon_1 d) + iZ_0 \tan(\beta_0 x)}{Z_0 + (A_c/\omega\varepsilon_1 d)\tan(\beta_0 x)} \right\}. \quad \text{A11}$$

Rearranging equation (A11) one obtains,

$$\frac{\varepsilon_1}{\varepsilon_0} = \frac{\lambda}{2\pi d} \left\{ \frac{(Z_0/Z_{\text{in}}) - i\tan(\beta_0 x)}{(Z_0/Z_{\text{in}})\tan(\beta_0 x) + i} \right\}. \quad \text{A12}$$

A4 Combined Method for Measuring Permeability and Permittivity

In the previous sections it was assumed that the sample thickness d was small compared to the wavelength within the sample. In the case of measuring the permeability, the sample was placed at the short-circuited end of a coaxial line where the effect of the electric field was considered to be negligible. This assumption breaks down when the sample depth becomes an appreciable fraction of the wavelength, which may happen at high frequencies and/or for materials which have a high dielectric constant such as water and

ferrites. When this happens it is no longer possible to determine μ independently of ε and vice versa and the necessity arises for a model which overcomes this deficiency. In this section we develop more general expressions for μ and ε.

For the short circuit termination, the load impedance is given by,

$$Z_{RSC} = Z_1 \tanh(\gamma_1 d) \qquad \text{A13}$$

and for the open circuited load,

$$Z_{ROC} = Z_1 \coth(\gamma_1 d) \qquad \text{A14}$$

Thus we have two equations for Z_1 and γ_1 and can calculate both μ and ε of the sample in the following manner.

Substituting eqns (A13) and (A14) into eqn (A1) and with, $Z_1 = A_c\sqrt{\mu_1/\varepsilon_1}$, one obtains the following,

$$Z_{insc} = Z_0\left\{\frac{A_c\sqrt{\mu_1/\varepsilon_1}\tanh(\gamma_1 d) + Z_0\tanh(\gamma_0 x)}{Z_0 + A_c\sqrt{\mu_1/\varepsilon_1}\tanh(\gamma_1 d)\tanh(\gamma_0 x)}\right\} \qquad \text{A15}$$

and

$$Z_{inoc} = Z_0\left\{\frac{A_c\sqrt{\mu_1/\varepsilon_1}\coth(\gamma_1 d) + Z_0\tanh(\gamma_0 x)}{Z_0 + A_c\sqrt{\mu_1/\varepsilon_1}\coth(\gamma_1 d)\tanh(\gamma_0 x)}\right\} \qquad \text{A16}$$

From eqns (A15) and (A16) one can obtain two expressions containing $\sqrt{\mu_1/\varepsilon_1}$ namely:

$$\sqrt{\frac{\mu_1}{\varepsilon_1}}\tanh(\gamma_1 d) = \frac{Z_0^2\tanh(\gamma_0 x) - Z_{insc}Z_0}{Z_{insc}A_c\tanh(\gamma_0 x) - Z_0 A_c} \qquad \text{A17}$$

And

$$\sqrt{\frac{\mu_1}{\varepsilon_1}}\coth(\gamma_1 d) = \frac{Z_0^2\tanh(\gamma_0 x) - Z_{inoc}Z_0}{Z_{inoc}A_c\tanh(\gamma_0 x) - Z_0 A_c}. \qquad \text{A18}$$

These equations can be further simplified by knowing that the characteristic impedance of the loss less part of the line is given by,

$$Z_0 = \frac{1}{2\pi}\ln\left(\frac{r_o}{r_i}\right)\sqrt{\frac{\mu_0}{\varepsilon_0}} = A_c\sqrt{\frac{\mu_0}{\varepsilon_0}}. \qquad \text{A19}$$

On using eqn (A19) in eqns (A17) and (A18) the line parameter, A_c, cancels out and dividing across by $\sqrt{\mu_0/\varepsilon_0}$ leaves

$$\sqrt{\frac{\mu_r}{\varepsilon_r}}\tanh(\gamma_1 d) = \frac{Z_0\tanh(\gamma_0 x) - Z_{insc}}{Z_{insc}\tanh(\gamma_0 x) - Z_0} \qquad \text{A20}$$

And

$$\sqrt{\frac{\mu_r}{\varepsilon_r}}\coth(\gamma_1 d) = \frac{Z_0\tanh(\gamma_0 x) - Z_{inoc}}{Z_{inoc}\tanh(\gamma_0 x) - Z_0}. \qquad \text{A21}$$

Multiplying eqn A20 by A21 one obtains μ_r/ε_r, where

$$\mu_r/\varepsilon_r = P + iQ = \frac{Z_0\tanh(\gamma_0 x) - Z_{insc}}{Z_{insc}\tanh(\gamma_0 x) - Z_0}\,x\,\frac{Z_0\tanh(\gamma_0 x) - Z_{inoc}}{Z_{inoc}\tanh(\gamma_0 x) - Z_0}. \qquad \text{A22}$$

P and *Q* denote the real and imaginary parts of the multiplication of the right hand sides of eqns (A20) and (A21).

Dividing eqn (A20) by (A21) results in,

$$\tanh^2(\gamma_1 d) = R + iS = \frac{Z_0\tanh(\gamma_0 x) - Z_{insc}}{Z_{insc}\tanh(\gamma_0 x) - Z_0}\,x\,\frac{Z_{inoc}\tanh(\gamma_0 x) - Z_0}{Z_0\tanh(\gamma_0 x) - Z_{inoc}}, \qquad \text{A23}$$

with *R* and *S* denoting the real and imaginary parts of the division exercise.

Inserting $\gamma_1 = i\omega\sqrt{\varepsilon_1\mu_1}$ into eqn (A23), and noting that $\tanh(i\theta) = i\tan\theta$, we obtain,

$$i\tan(\omega d\sqrt{\varepsilon_1\mu_1}) = \sqrt{R+iS}. \qquad \text{A24}$$

Solving for $\varepsilon_1\mu_1$, gives,

$$\varepsilon_1\mu_1 = \frac{1}{\omega^2 d^2}\left[\arctan\left(-i\sqrt{R+iS}\right)\right]^2 \qquad \text{A25}$$

Dividing A25 by $\varepsilon_0\mu_0$ gives the relative values, $\varepsilon_r\mu_r$ as

$$\varepsilon_r\mu_r = \frac{1}{\varepsilon_0\mu_0\omega^2 d^2}\left[\tan^{-1}\left(-i\sqrt{R+iS}\right)\right]^2 = X + iY. \qquad \text{A26}$$

Where,

$$X + iY = \frac{1}{\varepsilon_0\mu_0\omega^2 d^2}\left\{\tan^{-1}\left(-i\sqrt{\frac{Z_0\tanh(\gamma_0 x) - Z_{insc}}{Z_{insc}\tanh(\gamma_0 x) - Z_0}\,x\,\frac{Z_{inoc}\tanh(\gamma_0 x) - Z_0}{Z_0\tanh(\gamma_0 x) - Z_{inoc}}}\right)\right\}^2. \qquad \text{A27}$$

where *X* and *Y* represent the real and imaginary parts of the right hand side of eqn (A26). By combining eqns (A22) and (A26) one can solve for ε_r and μ_r. Firstly, if eqn (A22) is multiplied by eqn (A26), ε_r cancels out and one obtains,

$$\mu_r = \sqrt{(P+iQ)(X+iY)}. \qquad \text{A28}$$

If eqn (A26) is divided by eqn (A22) then μ_r cancels out one obtains,

$$\varepsilon_r = \sqrt{(X+iY)/(P+iQ)}. \qquad \text{A29}$$

Thus we have two equations for determining the complex permeability and permittivity, and all the parameters *P*, *Q*, *X* and *Y* can be determined from impedance measurements.

Further expanding (A28) and (A29) leads to,

$$\mu_r = \left\{\left(\frac{Z_0\tanh(\gamma_0 x) - Z_{insc}}{Z_{insc}\tanh(\gamma_0 x) - Z_0}\,x\,\frac{Z_0\tanh(\gamma_0 x) - Z_{inoc}}{Z_{inoc}\tanh(\gamma_0 x) - Z_0}\right)x\left[\frac{1}{\varepsilon_0\mu_0\omega^2 d^2}\left\{\tan^{-1}\left(-i\sqrt{\frac{Z_0\tanh(\gamma_0 x) - Z_{insc}}{Z_{insc}\tanh(\gamma_0 x) - Z_0}\,x\,\frac{Z_{inoc}\tanh(\gamma_0 x) - Z_0}{Z_0\tanh(\gamma_0 x) - Z_{inoc}}}\right)\right\}^2\right]\right\}^{\frac{1}{2}} \qquad \text{A30}$$

and

$$\varepsilon_r = \left\{\left(\frac{Z_0\tanh(\gamma_0 x) - Z_{insc}}{Z_{insc}\tanh(\gamma_0 x) - Z_0}\,x\,\frac{Z_0\tanh(\gamma_0 x) - Z_{inoc}}{Z_{inoc}\tanh(\gamma_0 x) - Z_0}\right)\div\left[\frac{1}{\varepsilon_0\mu_0\omega^2 d^2}\left\{\tan^{-1}\left(-i\sqrt{\frac{Z_0\tanh(\gamma_0 x) - Z_{insc}}{Z_{insc}\tanh(\gamma_0 x) - Z_0}\,x\,\frac{Z_{inoc}\tanh(\gamma_0 x) - Z_0}{Z_0\tanh(\gamma_0 x) - Z_{inoc}}}\right)\right\}^2\right]\right\}^{\frac{1}{2}}. \qquad \text{A31}$$

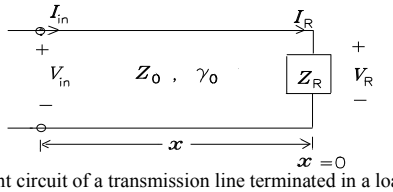

Fig 1. Equivalent circuit of a transmission line terminated in a load impedance Z_R. The line has a characteristic impedance Z_0, and propagation constant γ_0.

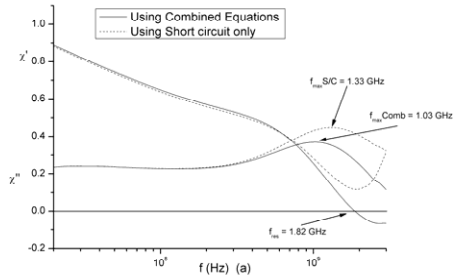

Fig.2. Plots of χ'(ω) and χ''(ω) for sample 1 in the frequency range 100 MHz to 3 GHz.

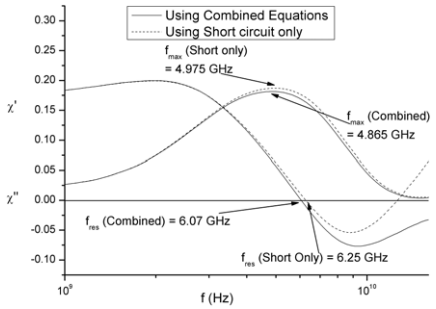

Fig.3. Plots of χ'(ω) and χ''(ω) for sample 2 in the frequency range 1 GHz to 16 GHz.

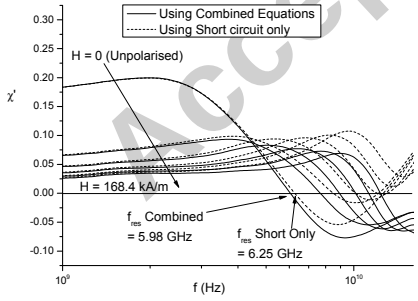

Fig. 4(a). Plots of χ'(ω) as a function of polarizing field, H, for sample 2 in the frequency range 1 GHz to 16 GHz.

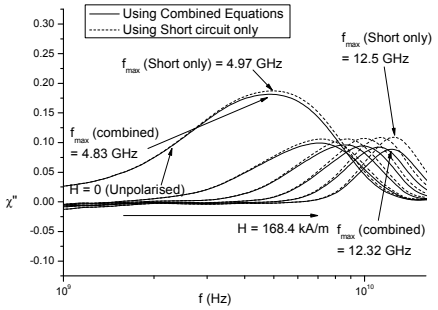

Fig.4 (b) Plots of $\chi''(\omega)$ as a function of polarizing field, H, for sample 2 in the frequency range 1 GHz to 16 GHz.

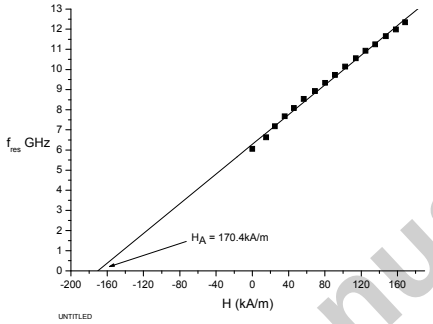

Fig.5. Plots of f_{res} as a function of polarizing field, H, for sample 2 in the range 0-164.5 kA/m.

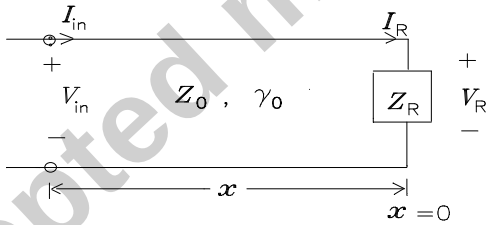

Fig 1(A). Equivalent circuit of a transmission line terminated in a load impedance, Z_R.